Dalton Transactions

COMMUNICATION

View Article Online
View Journal | View Issue

Cite this: *Dalton Trans.*, 2017, **46**, 11556

Received 12th June 2017,
Accepted 14th August 2017

DOI: 10.1039/c7dt02133j

rsc.li/dalton

Assembly of donor–acceptor hybrid heterostructures based on iodoplumbates and viologen coordination polymers†

Jian-Jun Liu,[a,b] Yue-Bin Shan,[a] Wen-Xin Dai,[a] Chang-Cang Huang*[a] and Mei-Jin Lin *[a]

The insertion of electron-rich iodoplumbate nanowires and nanolayers into layered electron-deficient metal-viologen frameworks leads to two donor–acceptor hybrid structures, respectively, which exhibit interesting semiconductor behaviors. Due to the bicontinuous donor and acceptor components, both of them exhibit highly efficient photocatalytic degradation activities over organic dyes under visible light irradiation compared to those of other iodoplumbate hybrid materials.

Inorganic–organic hybrid materials have been intensively investigated in the past few decades due to not only fascinating structural diversities for coordination chemistry and crystal engineering but also novel physical properties inherited from the interactions between inorganic and organic components.[1] Among hybrid functional materials, one of the most important families is organic–inorganic metal halides;[2] especially lead(II) iodide perovskite materials have received special attention since the Miyasaka group in 2009 reported the use of $CH_3NH_3PbI_3$ as a light absorber for photovoltaic cells.[3]

The optical and electrical properties of hybrid metal materials are mainly determined by the interplay between the negatively charged metal halide polyhedral complexes and the positively charged organic cations.[4] In most of these materials, the organic parts just acted as the counter ions to balance the negative charges of the inorganic moieties, rarely involved in functional organic components.[5] Recently, more and more attention has been paid to donor–acceptor hybrid materials, in which two functional components should possess different semiconductor properties.[6] It can be conceivable that the combination of donor components and acceptor components in one material is not only anticipated to form a unique heterostructure with synergetic properties, but also in favour of charge-carrier generation and separation.[7] However, the formation of such donor–acceptor structures is a difficult task that has long bedevilled scientists. Self-assembly is a promising strategy to organize donor and acceptor components into supramolecular architectures with periodically ordered donor–acceptor hybrid structures.[8] Iodoplumbates are well-known electron-donating semiconductors with diverse structures and tuneable energy levels.[4b,9] Due to the unsaturated coordination sites and electrostatic interactions, they should be an ideal candidate that could interact with electron-accepting organic moieties through coordination or host–guest interactions to form donor–acceptor hybrid structures. So far many hybrid complexes based on iodoplumbates and common organic components have been reported.[4a,9c,10] To our surprise, most of them are not bicontinuous.

It is well known that *N*,*N*′-disubstituted 4,4′-bipyridinium (viologen) and its derivatives are an attractive class of electron deficient molecules bearing an electrically charged moiety in their conjugation, which are ideal electron acceptors for the preparation of donor–acceptor hybrid semiconductors.[11] Although many groups have put most of their efforts into investigating coordination polymers and inorganic–organic hybrid complexes constructed from such viologen derivatives, few of them dealt with bicontinuous structures.[11a,12] In order to study the photoelectric properties, such bicontinuous donor–acceptor hybrid materials based on viologen complexes can be anticipated by rational design. Herein, we report two novel donor–acceptor hybrid complexes derived from electron-rich iodoplumbates and electron-deficient viologen coordination polymers, $[K_6Ni_2(BCEbpy)_4(H_2O)_{10}(Pb_9I_{30})]$ (**1**), $[Co(BCEbpy)(H_2O)_4]\cdot[Pb_3I_8]$ (**2**, BCEbpy = *N*,*N*′-bis(carboxyethyl)-4,4′-bipyridinium), which indeed possess unique bicontinuous heterostructures and exhibit semiconductive and photocatalytic properties.

In a straight glass tube, upon slow diffusion of a solution of nickel acetate (cobalt acetate for **2**) in methanol into a solution of PbI_2 and BCEbpy in saturated potassium iodide solution

[a]*State Key Laboratory of Photocatalysis on Energy and Environment, College of Chemistry, Fuzhou University, 350116, China. E-mail: meijin_lin@fzu.edu.cn, cchuang@fzu.edu.cn*

[b]*Center for Yunnan-Guizhou Plateau Chemical Functional Materials and Pollution Control, Qujing Normal University, 655011, China*

†Electronic supplementary information (ESI) available: Experimental details, TGA and PXRD plots, crystallographic data (CIF), UV-Vis spectra and other figures. CCDC 1545737 and 1545738. For ESI and crystallographic data in CIF or other electronic format see DOI: 10.1039/c7dt02133j

with a buffered layer mixture solution of MeOH and H_2O (1 : 1 in volume), dark red plate-like crystals of **1** (dark red block crystals for **2**) were obtained after a week in the dark. The purity of these crystalline products was examined by PXRD (Fig. S9 and S10, ESI†), revealing that almost only one phase was formed for **1** and **2** because of the good fit between their simulated and observed patterns.

Single crystal X-ray analysis reveals that **1** crystallizes in the monoclinic space group $C2/m$, and consists of a cationic framework host and an anionic iodoplumbate guest motif (Fig. 1). For the cationic framework motif, each nickel cation adopts an octahedral geometry coordinated with four O atoms from four BCEbpy tectons in the square plane (d_{Ni-O} = 2.022–2.061 Å) and two water molecules in the axial positions (d_{Ni-O} = 2.093–2.107 Å) to yield a mononuclear complex, which is further bridged by BCEbpy linkers to form a cationic two-dimensional framework with a square grid of 16.6 × 16.6 Å (Fig. 1a). Along the c axis, the two neighbouring networks are slightly slipped to form a three-dimensional supramolecular framework (Fig. 1b).

For the anionic guest motif, it is an infinite one-dimensional iodoplumbate wire with the formula of $(Pb_9I_{30})_n^{12n-}$ (Fig. 1c). In iodoplumbate wires, there are three crystallographically independent Pb atoms, each Pb atom is surrounded by six I atoms and situated in a slightly distorted octahedral coordination environment. The PbI_6 octahedron is connected by edge-sharing and face-sharing modes to give a $Pb_9I_{30}^{12-}$ unit. Similarly, three kinds of iodine atoms can also be observed in each $Pb_9I_{30}^{12-}$ unit, which are terminal μ_1-I, bridged μ_2-I, and μ_3-I, respectively. The adjacent $Pb_9I_{30}^{12-}$ units are further linked by μ_2-I to generate a one-dimensional nanowire with a width of 10.2 Å (Fig. 1c). The bond lengths of Pb–I fall in the range of 3.083–3.410 Å with an average value of 3.212 Å, reasonable for Pb cations in iodoplumbates.[13] The one-dimensional iodoplumbate nanowire is linked to the cationic framework motif through the K–I bond (3.483–3.837 Å, Fig. S2, ESI†) between the I atom of the iodoplumbate nanowire and the K atom of the host framework (Fig. 1d and e) to form the final inorganic–organic hybrids with iodoplumbate nanowires loaded in the three-dimensional supramolecular framework.

Different from the case for **1**, **2** crystallizes in the triclinic space group $P\bar{1}$, and consists of a cationic two-dimensional supramolecular framework and an anionic two-dimensional iodoplumbate motif. There are one and a half of Pb(II) cations, a half of a Co(II) cation, four I^- anions, a half of a BCEbpy tecton and two coordinated water molecules in the asymmetric unit of **2**. In this structure, the Co(II) cation is six-coordinated by four water molecules and two O atoms from two independent BCEbpy tectons in monodentate modes, which is further bridged by BCEbpy linkers to form a one-dimensional chain (Fig. 2a). Through C6–H6B···O2 hydrogen bonding, the one-dimensional chains are linked to generate two-dimensional supramolecular layers in the ac plane, of which the distance is 2.984 Å (Fig. 2c). For the iodoplumbate motif, there are two independent Pb sites, each Pb cation is surrounded by six I atoms and situated in a slightly distorted octahedral coordination environment. The adjacent PbI_6 octahedra are connected by edge-sharing mode to give a two-dimensional iodoplumbate layer (Fig. 2b). These two-dimensional iodoplumbate layers are stacked with the above-mentioned two-dimensional supramolecular layers by C5–H5···I1 hydrogen bonding interactions to form a 3D inorganic–organic hybrid architecture (Fig. 2d).

The solid-state optical diffuse reflection spectra of **1** and **2** were measured at room temperature and their band gaps were calculated from the diffuse reflectance data by using the Kubelka–Munk function. The band gaps of **1** and **2** are found to be 1.89 and 1.83 eV, respectively (Fig. S8, ESI†), which are in accordance with their dark red appearance. Pure inorganic iodoplumbates are usually wide band gap semiconductors,[14]

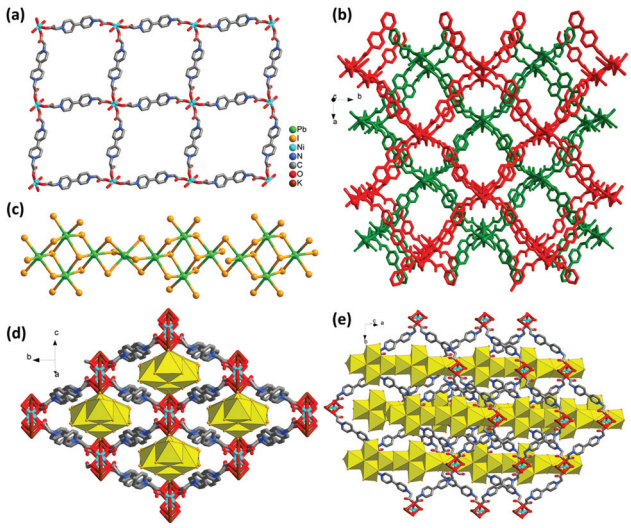

Fig. 1 Portions of the X-ray structures of **1** showing (a) the 2D laminar networks; (b) staggered grid of the host framework motif; (c) anionic $(Pb_9I_{30})_n^{12n-}$ nanowire; (d) and (e) the packing diagram of **1** viewed along different directions. Coordination spheres of Pb atoms are shown as polyhedra in (d) and (e) for clarity.

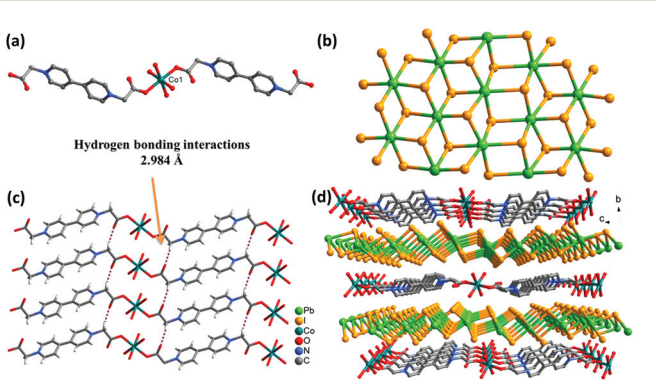

Fig. 2 (a) Coordination environment of Co^{2+} in **2**; (b) layered structure of $(Pb_3I_8)_n^{2n-}$; (c) two-dimensional hydrogen bonding network; (d) packing diagram of **2** viewed along the a direction.

however, the interactions between organic ligands and the iodoplumbate can affect the energy levels near the Fermi level, which make such hybrids potential narrow-band-gap semiconductors.

The narrow band gaps of the compounds encouraged us to investigate their visible light photocatalytic activities, which were evaluated by the degradation of Rhodamine B (RhB) as the test pollutant under visible light irradiation at room temperature. 50 mg catalyst powders were suspended in 50 mL of RhB solution (concentration: 10^{-5} mol L^{-1}), and then they were magnetically stirred in the dark for 10 min to ensure the equilibrium of adsorption/desorption. Afterwards, under the irradiation of a 300 W xenon lamp, the solution was continuously kept under stirring with the aid of a magnetic stirrer. A 3.0 mL sample was taken for analysis every 5 min. The time dependent absorption spectra of RhB degraded with samples **1** and **2** are as shown in Fig. 3. The degradation efficiency is defined as C/C_0, where C and C_0 represent the remnant and initial concentrations of RhB, respectively. For sample **1**, the degradation ratio of RhB reached nearly 100% after irradiation for 20 min, resulting in complete decolorization. Such a phenomenon is also demonstrated by the change in the color of the dispersion from an initial red to colorless (Fig. S12, ESI†). Compared with **1**, sample **2** shows slightly lower photocatalytic activity and it can completely decompose the RhB within 25 min. At the same time, a control experiment was also accomplished under the same conditions without any catalysts, and the result shows that the RhB self-photodegradation is almost negligible (Fig. S11, ESI†). Furthermore, we also studied their recycling performances and found only slight decay (about 5%) in the catalytic efficiencies over three cycles (Fig. S12 and S13, ESI†). After photocatalysis, the PXRD patterns of **1** and **2** were still in agreement with the original patterns (Fig. S9 and S10, ESI†), which indicate the unchanged basic structures as well as the stabilities of **1** and **2** as the visible light responding photocatalysts.

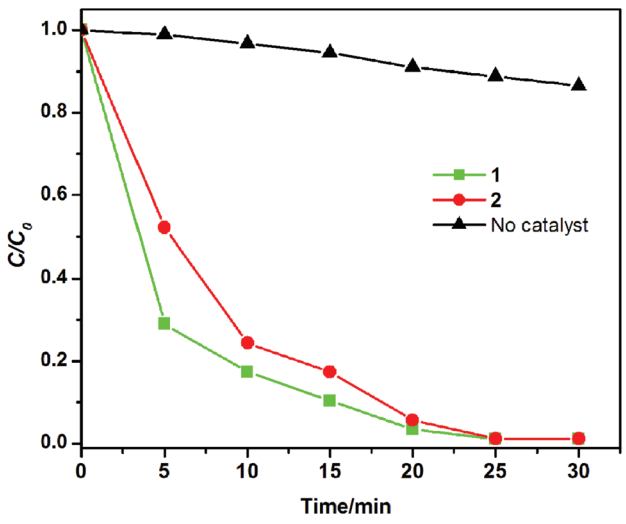

Fig. 3 Concentration change of RhB irradiated under a 300 W xenon lamp as a function of irradiation time with or without the presence of **1** and **2**, C and C_0 stand for the RhB concentrations after and before irradiation.

Compared to the photocatalytic activities of the reported iodoplumbate-based hybrid complexes,[15] those of **1** and **2** are found to increase significantly, which may be attributed to their bicontinuous donor–acceptor heterostructures. As far as we know, metal halides are generally used as electron donors in photocatalysis. In the complexes **1** and **2**, the photogenerated electrons are able to easily transfer from the continuous iodoplumbates to the electron-deficient viologen motif under light illumination. At the same time, the holes are transferred to the iodoplumbates, which are used for the oxidation of RhB. In the viologen motif, the obtained electrons are expected to be trapped by O_2 in the solution to form superoxide ions and other reactive oxygen species.[16] Accordingly, the continuous 2D electron-deficient frameworks in **1** and **2** are able to effectively accept and transfer photogenerated electrons to avoid electron–hole recombination, which is supposed to answer for their improved degradation efficiency of RhB.

In conclusion, we have demonstrated that the insertion of electron-rich iodoplumbate nanowires and nanolayers into two layered electron-deficient metal-viologen frameworks led to two novel donor–acceptor hybrid materials, which exhibit interesting narrow-band-gap semiconductor behaviours and high photocatalytic degradation activities over organic dyes under visible light irradiation. The high photocatalytic activities are attributed to their unique bicontinuous donor–acceptor structural features. We envision that such work will contribute not only to the basic science of hybrid materials but would also be used towards high-performance photovoltaics and molecular electronics.

Conflicts of interest

There are no conflicts to declare.

Acknowledgements

This work has been supported by the National Natural Science Foundation of China (21572032) and the Program for New Century Excellent Talents in Fujian Province University.

Notes and references

1 (*a*) R. Pardo, M. Zayat and D. Levy, *Chem. Soc. Rev.*, 2011, **40**, 672–687; (*b*) C. Bellitto, E. M. Bauer and G. Righini, *Coord. Chem. Rev.*, 2015, **289–290**, 123–136; (*c*) O. Fuhr, S. Dehnen and D. Fenske, *Chem. Soc. Rev.*, 2013, **42**, 1871–1906; (*d*) J. Zhou, J. Dai, G. Q. Bian and C. Y. Li, *Coord. Chem. Rev.*, 2009, **253**, 1221–1247; (*e*) Q. Gong, Z. Hu, B. J. Deibert, T. J. Emge, S. J. Teat, D. Banerjee, B. Mussman, N. D. Rudd and J. Li, *J. Am. Chem. Soc.*, 2014,

136, 16724–16727; (*f*) R.-G. Lin, G. Xu, M.-S. Wang, G. Lu, P.-X. Li and G.-C. Guo, *Inorg. Chem.*, 2013, **52**, 1199–1205.

2 (*a*) G.-E. Wang, G. Xu, M.-S. Wang, L.-Z. Cai, W.-H. Li and G.-C. Guo, *Chem. Sci.*, 2015, **6**, 7222–7226; (*b*) X.-W. Lei, C.-Y. Yue, J.-Q. Zhao, Y.-F. Han, J.-T. Yang, R.-R. Meng, C.-S. Gao, H. Ding, C.-Y. Wang and W.-D. Chen, *Cryst. Growth Des.*, 2015, **15**, 5416–5426; (*c*) X.-W. Lei, C.-Y. Yue, J.-Q. Zhao, Y.-F. Han, J.-T. Yang, R.-R. Meng, C.-S. Gao, H. Ding, C.-Y. Wang, W.-D. Chen and M.-C. Hong, *Inorg. Chem.*, 2015, **54**, 10593–10603; (*d*) J. Shen, C. Zhang, T. Yu, L. An and Y. Fu, *Cryst. Growth Des.*, 2014, **14**, 6337–6342; (*e*) J.-J. Shen, X.-X. Li, T.-L. Yu, F. Wang, P.-F. Hao and Y.-L. Fu, *Inorg. Chem.*, 2016, **55**, 8271–8273.

3 (*a*) A. Kojima, K. Teshima, Y. Shirai and T. Miyasaka, *J. Am. Chem. Soc.*, 2009, **131**, 6050–6051; (*b*) G. E. Eperon, S. D. Stranks, C. Menelaou, M. B. Johnston, L. M. Herz and H. J. Snaith, *Energy Environ. Sci.*, 2014, **7**, 982–988; (*c*) K. Yan, M. Long, T. Zhang, Z. Wei, H. Chen, S. Yang and J. Xu, *J. Am. Chem. Soc.*, 2015, **137**, 4460–4468; (*d*) H. Zhou, Q. Chen, G. Li, S. Luo, T. Song, H.-S. Duan, Z. Hong, J. You, Y. Liu and Y. Yang, *Science*, 2014, **345**, 542–546; (*e*) J. H. Heo, H. J. Han, D. Kim, T. K. Ahn and S. H. Im, *Energy Environ. Sci.*, 2015, **8**, 1602–1608; (*f*) S. S. Shin, E. J. Yeom, W. S. Yang, S. Hur, M. G. Kim, J. Im, J. Seo, J. H. Noh and S. I. Seok, *Science*, 2017, **356**, 167–171.

4 (*a*) L.-M. Wu, X.-T. Wu and L. Chen, *Coord. Chem. Rev.*, 2009, **253**, 2787–2804; (*b*) N. Mercier, N. Louvain and W. Bi, *CrystEngComm*, 2009, **11**, 720–734; (*c*) N. Leblanc, W. Bi, N. Mercier, P. Auban-Senzier and C. Pasquier, *Inorg. Chem.*, 2010, **49**, 5824–5833.

5 (*a*) B. Saparov and D. B. Mitzi, *Chem. Rev.*, 2016, **116**, 4558–4596; (*b*) J. Zhou, J. Dai, G. Q. Bian and C. Y. Li, *Coord. Chem. Rev.*, 2009, **253**, 1221–1247; (*c*) M.-S. Wang, G. Xu, Z.-J. Zhang and G.-C. Guo, *Chem. Commun.*, 2010, **46**, 361–376; (*d*) N. Leblanc, M. Allain, N. Mercier and L. Sanguinet, *Cryst. Growth Des.*, 2011, **11**, 2064–2069; (*e*) S. Eppel, N. Fridman and G. Frey, *Cryst. Growth Des.*, 2015, **15**, 4363–4371; (*f*) T. Yu, L. An, L. Zhang, J. Shen and Y. Fu, *Cryst. Growth Des.*, 2014, **14**, 3875–3879.

6 (*a*) G. Yu, J. Gao, J. C. Hummelen, F. Wudi and A. J. Heeger, *Science*, 1995, **270**, 1789–1791; (*b*) R. Pandey and R. J. Holmes, *Adv. Mater.*, 2010, **22**, 5301–5305; (*c*) A. Tada, Y. Geng, Q. Wei, K. Hashimoto and K. Tajima, *Nat. Mater.*, 2011, **10**, 450–455; (*d*) H. Zheng, Y. Li, H. Liu, X. Yin and Y. Li, *Chem. Soc. Rev.*, 2011, **40**, 4506–4524; (*e*) S. Prasanthkumar, S. Ghosh, V. C. Nair, A. Saeki, S. Seki and A. Ajayaghosh, *Angew. Chem., Int. Ed.*, 2015, **54**, 946–950.

7 (*a*) Y. Huang, E. J. Kramer, A. J. Heeger and G. C. Bazan, *Chem. Rev.*, 2014, **114**, 7006–7043; (*b*) A. Kira, T. Umeyama, Y. Matano, K. Yoshida, S. Isoda, J. K. Park, D. Kim and H. Imahori, *J. Am. Chem. Soc.*, 2009, **131**, 3198–3200; (*c*) A. Mishra and P. Bäuerle, *Angew. Chem., Int. Ed.*, 2012, **51**, 2020–2067; (*d*) I. C. Smith, E. T. Hoke, D. Solis-Ibarra, M. D. McGehee and H. I. Karunadasa, *Angew. Chem., Int. Ed.*, 2014, **53**, 11232–11235.

8 (*a*) S. Jin, X. Ding, X. Feng, M. Supur, K. Furukawa, S. Takahashi, M. Addicoat, M. E. El-Khouly, T. Nakamura, S. Irle, S. Fukuzumi, A. Nagai and D. Jiang, *Angew. Chem., Int. Ed.*, 2013, **52**, 2017–2021; (*b*) X.-L. Hu, C.-Y. Sun, C. Qin, X.-L. Wang, H.-N. Wang, E.-L. Zhou, W.-E. Li and Z.-M. Su, *Chem. Commun.*, 2013, **49**, 3564–3566; (*c*) L. Chen, K. Furukawa, J. Gao, A. Nagai, T. Nakamura, Y. Dong and D. Jiang, *J. Am. Chem. Soc.*, 2014, **136**, 9806–9809; (*d*) W.-W. Xiong, J. Miao, K. Ye, Y. Wang, B. Liu and Q. Zhang, *Angew. Chem., Int. Ed.*, 2015, **54**, 546–550; (*e*) F. Wang, Z.-S. Liu, H. Yang, Y.-X. Tan and J. Zhang, *Angew. Chem., Int. Ed.*, 2011, **50**, 450–453.

9 (*a*) L. Pedesseau, J.-M. Jancu, A. Rolland, E. Deleporte, C. Katan and J. Even, *Opt. Quantum Electron.*, 2014, **46**, 1225–1232; (*b*) Y. Zhao and K. Zhu, *Chem. Soc. Rev.*, 2016, **45**, 655–689; (*c*) V. Gómez, O. Fuhr and M. Ruben, *CrystEngComm*, 2016, **18**, 8207–8219; (*d*) Z. Chen, Z.-G. Gu, W.-Q. Fu, F. Wang and J. Zhang, *ACS Appl. Mater. Interfaces*, 2016, **8**, 28737–28742.

10 (*a*) L.-Q. Fan, L.-M. Wu and L. Chen, *Inorg. Chem.*, 2006, **45**, 3149–3151; (*b*) S. Mishra, E. Jeanneau, S. Daniele, G. Ledoux and P. N. Swamy, *Inorg. Chem.*, 2008, **47**, 9333–9343; (*c*) H.-H. Li, Y.-L. Wu, H.-J. Dong, M. Wang, S.-W. Huang and Z.-R. Chen, *CrystEngComm*, 2011, **13**, 6766–6773; (*d*) S.-P. Zhao and X.-M. Ren, *Dalton Trans.*, 2011, **40**, 8261–8272; (*e*) Z. J. Zhang, S. C. Xiang, G. C. Guo, G. Xu, M. S. Wang, J. P. Zou, S. P. Guo and J. S. Huang, *Angew. Chem., Int. Ed.*, 2008, **47**, 4149–4152; (*f*) A. Guloy, Z. Tang, P. Miranda and V. Srdanov, *Adv. Mater.*, 2001, **13**, 833–837; (*g*) H.-H. Li, Z.-R. Chen, L.-C. Cheng, J.-B. Liu, X.-B. Chen and J.-Q. Li, *Cryst. Growth Des.*, 2008, **8**, 4355–4358.

11 (*a*) J.-K. Sun and J. Zhang, *Dalton Trans.*, 2015, **44**, 19041–19055; (*b*) X.-L. Sun, Q.-Y. Zhu, W.-Q. Mu, L.-W. Qian, L. Yu, J. Wu, G.-Q. Bian and J. Dai, *Dalton Trans.*, 2014, **43**, 12582–12589; (*c*) D. Kiriya, M. Tosun, P. Zhao, J. S. Kang and A. Javey, *J. Am. Chem. Soc.*, 2014, **136**, 7853–7856; (*d*) D. Aulakh, J. R. Varghese and M. Wriedt, *Inorg. Chem.*, 2015, **54**, 1756–1764; (*e*) H.-Y. Li, H. Xu, S.-Q. Zang and T. C. W. Mak, *Chem. Commun.*, 2016, **52**, 525–528; (*f*) J.-J. Liu, Y.-F. Guan, M.-J. Lin, C.-C. Huang and W.-X. Dai, *Cryst. Growth Des.*, 2016, **16**, 2836–2842.

12 (*a*) P.-X. Li, M.-S. Wang, M.-J. Zhang, C.-S. Lin, L.-Z. Cai, S.-P. Guo and G.-C. Guo, *Angew. Chem., Int. Ed.*, 2014, **53**, 11529–11531; (*b*) J.-J. Liu, Y.-F. Guan, M.-J. Lin, C.-C. Huang and W.-X. Dai, *Cryst. Growth Des.*, 2015, **15**, 5040–5046; (*c*) Y. Chen, Z.-O. Wang, Z. Yang, Z.-G. Ren, H.-X. Li and J.-P. Lang, *Dalton Trans.*, 2010, **39**, 9476–9479; (*d*) Z. Tang and A. M. Guloy, *J. Am. Chem. Soc.*, 1999, **121**, 452–453; (*e*) J.-J. Liu, Y.-F. Guan, L. Li, Y. Chen, W.-X. Dai, C.-C. Huang and M.-J. Lin, *Chem. Commun.*, 2017, **53**, 4481–4484; (*f*) G. Xu, G.-C. Guo, M.-S. Wang, Z.-J. Zhang, W.-T. Chen and J.-S. Huang, *Angew. Chem., Int. Ed.*, 2007, **46**, 3249–3251.

13 (*a*) N. Louvain, N. Mercier, J. Luc and B. Sahraoui, *Eur. J. Inorg. Chem.*, 2008, 3592–3596; (*b*) G.-E. Wang, X.-M. Jiang, M.-J. Zhang, H.-F. Chen, B.-W. Liu, M.-S. Wang and G.-C. Guo, *CrystEngComm*, 2013, **15**, 10399–10404; (*c*) H.-B. Duan, S.-S. Yu, Y.-B. Tong, H. Zhou and X.-M. Ren, *Dalton Trans.*, 2016, **45**, 4810–4818.

14 (*a*) X. H. Zhu, Z. R. Wei, Y. R. Jin and A. P. Xiang, *Cryst. Res. Technol.*, 2007, **42**, 456–459; (*b*) J.-P. Li, L.-H. Li, L.-M. Wu and L. Chen, *Inorg. Chem.*, 2009, **48**, 1260–1262.

15 (*a*) G.-N. Liu, J.-R. Shi, X.-J. Han, X. Zhang, K. Li, J. Li, T. Zhang, Q.-S. Liu, Z.-W. Zhang and C. Li, *Dalton Trans.*, 2015, **44**, 12561–12575; (*b*) C.-H. Wang, H.-J. Du, Y. Li, Y.-Y. Niu and H.-W. Hou, *New J. Chem.*, 2015, **39**, 7372–7378.

16 (*a*) M. R. Hoffmann, S. T. Martin, W. Choi and W. Bahnemann, *Chem. Rev.*, 1995, **95**, 69–96; (*b*) E. J. Nanni Jr., C. T. Angelis, J. Dickson and D. T. Sawyer, *J. Am. Chem. Soc.*, 1981, **103**, 4268–4270.